Superconductor-to-normal phase transition in a vortex glass model: numerical evidence for a new percolation universality class

Frank O Pfeiffer and Heiko Rieger

Theoretische Physik, Universität des Saarlandes, 66041 Saarbrücken, Germany

Abstract
The three-dimensional strongly screened vortex glass model is studied numerically using methods from combinatorial optimization. We focus on the effect of disorder strength on the ground state and find the existence of a disorder-driven normal-to-superconducting phase transition. The transition turns out to be a geometrical phase transition with percolating vortex loops in the ground state configuration. We determine the critical exponents and provide evidence for a new universality class of correlated percolation.

(Some figures in this article are in colour only in the electronic version)

1. Introduction

The gauge glass model is a paradigmatic model for disordered arrays of Josephson junctions or amorphous granular superconductors [1]. It has been argued that it also describes the relevant physics of the superconductor-to-normal phase transition in high-T_c superconductors [2]. A powerful tool for investigating this transition is the domain wall renormalization group (DWRG) technique that has been applied successfully to this model [3–6]: in essence one calculates the stiffness of the system with respect to twisting the phase variables at opposite boundaries of a system of linear size L. If the twist costs an energy that increases with L one can conclude that the system is superconducting, if it decreases, one concludes that the phase coherence necessary for superconductivity is destroyed by thermal fluctuations, i.e. the system is in a normal phase. In this paper we study this model in the strong screening limit with varying disorder strengths at zero temperature. We will find a superconductor-to-normal transition (at $T = 0$) at a critical disorder strength and show that it is accompanied by a proliferation of disorder-induced global vortex loops. By a finite-size scaling analysis of the loop statistics we show that it is a percolation transition of a novel universality class.

This paper is structured as follows: in section 2 we present the model which predicts a disorder-driven phase transition using the concept of defect energy. In the next two sections our results are presented. Section 3 shows a clear phase transition with the study of an excitation

loop perturbation. In section 4 we show the transition to be a geometrical phase transition, which allows us to apply percolation theory to the vortex glass model. The critical probability above which a loop percolates, the critical exponents and the scaling relations are calculated numerically. We close with a summary in section 5.

2. Model

The gauge glass model [4, 6] is a phenomenological lattice model describing the phase fluctuations in a granular disordered superconductor close to the normal-to-superconducting phase transition

$$\mathcal{H} = -J \sum_{\langle ij \rangle} \cos(\phi_i - \phi_j - A_{ij} - \lambda^{-1} a_{ij}) + \tfrac{1}{2} \sum_{\square} (\nabla \times \boldsymbol{a})^2 \qquad (1)$$

where J is the effective coupling (set to 1) and ϕ_i the phase on site i. The sum is over all nearest neighbours $\langle ij \rangle$ on a simple cubic lattice of system size L with periodic boundary conditions. A_{ij} are the vector potentials, which are uniformly distributed on

$$A_{ij} \in [0, 2\pi \sigma] \qquad \text{with a fixed} \quad \sigma \in [0, 1] \qquad (2)$$

where σ defines the disorder strength. $\sigma = 1$ corresponds to strong disorder and $\sigma = 0$ to the pure system. λ is the bare screening length. The fluctuating vector potentials a_{ij} are integrated over $-\infty$ to ∞ subject to $\nabla \cdot \boldsymbol{a} = 0$. The last term in (1) describes the magnetic energy and its sum is over all elementary plaquettes of the lattice. To investigate the gauge glass model in the strong screening limit $\lambda \to 0$ we make use of the vortex representation [7], which gives after standard manipulations [4]

$$\mathcal{H}_V^{\lambda \to 0} = \tfrac{1}{2} \sum_i (\boldsymbol{n}_i - \boldsymbol{b}_i)^2 \qquad \text{with the magnetic field} \quad \boldsymbol{b}_i = \frac{1}{2\pi} \sum_{\square} A_{ij} \quad (3)$$

subject to the local constraint $(\nabla \cdot \boldsymbol{n})_i = 0$. The computation of the ground state of the Hamiltonian (3), i.e. the vortex configuration $\boldsymbol{n}$ with the lowest energy $\mathcal{H}_V(\boldsymbol{n})$, is a minimum cost flow problem that can be solved *exactly* in polynomial time with appropriate combinatorial optimization algorithms [8].

We use the defect energy scaling method to show that there is a superconducting-to-normal phase transition at low temperature T varying the strength of disorder σ. The idea is to calculate the energy ΔE necessary to introduce a low-energy excitation loop (or domain wall) of size L into the system. We generate the excitation loop by a global manipulation of the energy couplings along a fixed direction, as described in detail in [6,9]. The defect energy ΔE results from the difference energy of the ground state with and without a global excitation loop. Its disorder average is assumed to scale with the system size L as

$$\Delta E \sim L^{\theta}. \qquad (4)$$

The sign of the stiffness exponent θ determines whether the ground state is stable with respect to thermal fluctuations. If $\theta > 0$ it costs an infinite amount of energy to induce a domain wall crossing an infinite system ($L \to \infty$) and therefore the the ground state remains stable at small but non-vanishing temperatures: there is an ordered low-temperature phase, as in a $3d$ XY-ferromagnet. On the other hand, if $\theta < 0$ arbitrarily large excitations loops cost less and less energy: the ground state is unstable and thus is not an ordered phase at any non-vanishing temperatures, like in a $2d$ XY spin glass.

We can easily see from (3) that for small disorder (i.e. small σ) the ground state is simply $\boldsymbol{n} = 0$ and $\theta = 1$: for a given disorder strength σ, it is $b_i \in [-2\sigma, 2\sigma]$. Thus, as long as $\sigma < 1/4$, $|b_i| < 1/2$ and the absolute minimum of all terms $(\boldsymbol{n}_i - \boldsymbol{b}_i)^2$ occurring in the
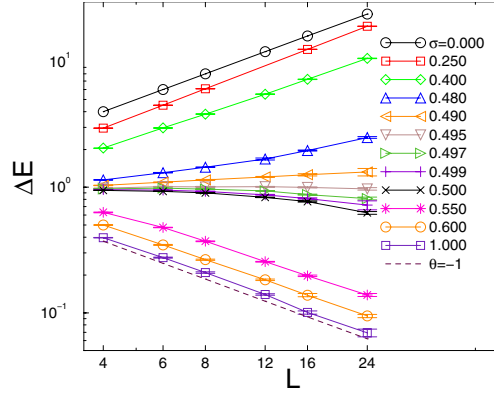
Figure 1. Log–log plot of the disorder-averaged defect energy ΔE versus system size L for different disorder strengths σ and sample sizes N_{samp}. For $L = 4, 6, 8$ we used $N_{\mathrm{samp}} = 20\,000$, for $L = 12$ $N_{\mathrm{samp}} = 5000$, for $L = 16$ $N_{\mathrm{samp}} = 1000$ and for $L = 24$ $N_{\mathrm{samp}} = 500$.

Hamiltonian (3) fulfilling the constraint that n_i has to be an integer is $n_i = 0$. A global excitation loop contains at least L bonds with $n_i = 1$, which implies that for $\sigma < 1/4$ an additional global excitation loop would cost a defect energy $\Delta E \propto L$. This implies a stiffness exponent $\theta = 1$ for small disorder, certainly for $\sigma < 1/4$, possibly even for larger σ as we will see below. Thus we can already at this point conclude that for weak disorder the system described by (3) is superconducting (or ferromagnetic in the the magnetic XY language), as it is in the pure case ($\sigma = 0$).

On the other hand, in the opposite limit of strong disorder, $\sigma = 1$, defect energy calculations [6,9] gave a negative stiffness exponent $\theta = -0.96 \pm 0.05$, indicating the absence of an ordered low-temperature phase (in particular the absence of a stable low-temperature vortex glass phase [10]). Therefore one can expect a disorder-driven phase transition at zero temperature from a superconducting phase for weak disorder to a normal phase for strong disorder. We expect that this transition takes place at a critical disorder strength σ_c ($\sigma_c > 1/4$ from what we said above) and is characterized by a discontinuous jump of the stiffness exponent θ from 1 to -0.96 (here we assume the simplest scenario in which one has only two attracting zero-temperature fixed points besides the critical point σ_c).

3. Defect energy

Figure 1, showing the defect energy ΔE versus system size L in a log–log plot, demonstrates that our numerical results confirm the scenario described above. The slopes of the different curves, representing different disorder strengths σ, are identical to the stiffness exponent θ. We observe that around $\sigma_c = 0.495 \pm 0.005$ it jumps from positive to negative with increasing σ, this is our estimate for the location of the disorder-driven transition from the superconducting to the normal phase. Note that for the unscreened gauge glass XY model it was found that $\sigma_c \approx 0.55$ [5].

In what follows we will show that this zero-temperature transition is actually a second-order phase transition characterized by a single length scale diverging at σ_c. This length scale corresponds to the average diameter of closed loops in the ground state and at σ_c these loops percolate the infinite system (note that we have periodic boundary conditions) (see figure 2). Thus what actually happens at σ_c is a percolation transition of vortex loops in the ground state, and in order to estimate its critical exponents we will now perform a finite-size scaling analysis of the critical behaviour.
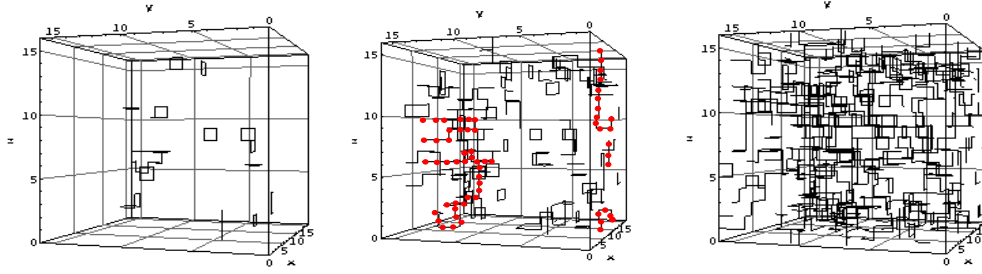
Figure 2. Three ground state configurations for growing disorder strengths $\sigma = 0.45$ (left), 0.50 (middle) and 0.55 (right), respectively, and system size $L = 16$. At $\sigma = 0.50$ a percolating loop appears (dotted line).

4. Vortex loop percolation transition

First we note that at σ_c the concentration of vortex variables that are non-zero ($n_i \neq 0$), i.e. the probability p with which a bond in the simple cubic lattice is occupied with a vortex segment, turns out to be $p_c = 0.033 \pm 0.005$. This value is much lower than the percolation threshold for conventional bond percolation on the simple cubic lattice [11], which is $p_c^{\text{perco}} \approx 0.249$ [12]. This is a consequence of the global constraint (divergence-free) underlying the optimization problem (3), which obviously causes strong correlations in the bond occupation process. Hence we suspect that the transition we are considering establishes a new percolation universality class[1].

The geometrical objects of the ground state n of model (3) that we are going to study are *loops*. The algorithm to detect loops is the following:

given the ground state configuration n;

while it exists a vortex segment with $n_i \neq 0$ along the bond i do:

(I) choose i;

(II) find the shortest path P_i along non-zero vortex segments from the target site of i to the source site of i, where the direct path along i is excluded;

(III) calculate $flow := \sum_{j \in P_i \cup \{i\}} n_j$: if $flow \neq 0$ or if there are two occupied bonds in a distance L or greater along the x, y or z direction, which belong to the same loop, then the loop is called a *global* loop else a *local* loop;

(IV) cancel the detected loop $P_i \cup \{i\}$ and continue the *while* loop.

For each system with $L = 4, 6, 8, 10, 12$ and 16 we calculated 2000 different samples, and for $L = 20, 24$ and 32 we calculated 1000 samples and then analysed the loop statistics.

By studying the probability $P_L^{\text{perco}}(\sigma)$ that a system of linear size L contains at least one percolating loop we can check, whether the percolation transition does indeed coincide with the jump in the stiffness exponent located above. Its finite-size scaling form is given by

$$P_L^{\text{perco}}(p) = \tilde{P}^{\text{perco}}[(\sigma - \sigma_c)L^{1/\nu}] \tag{5}$$

thus it is independent of system size at σ_c and curves for different system sizes should intersect. Our data are shown in the inset of figure 3 (left) and we locate the intersection point

$$\sigma_c = 0.492 \pm 0.005 \tag{6}$$

agreeing well with our estimate for σ_c from the defect energy analysis.

---

[1] A different loop percolation transition happens in plaquette percolation, in which randomly, with probabiliy p, the elementary plaquettes of a simple cubic lattice are occupied, the four boundary sides forming an elementary loop. Here the optimization constraint coming from the Hamiltonian (3) is missing, giving rise to a different universality class from the one considered here.
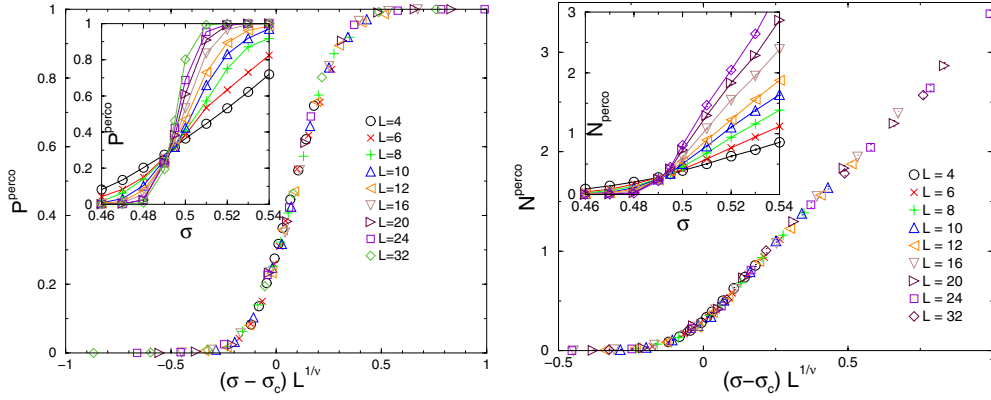
Figure 3. Finite-size scaling of the percolation probability P^{perco} (left) and the average number N_{perco} of percolating loops (right) for different system sizes L with $\sigma_c = 0.492$ and $\nu = 1.05$. The inset shows the raw data. The error bars are smaller than the symbol size and are therefore omitted.

Next we deduce an estimate for the correlation length exponent ν by plotting $P_L^{\text{perco}}(p)$ versus $(\sigma - \sigma_c)L^{1/\nu}$, where we fix σ_c and determine ν such as to achieve the best data collapse. This is done in figure 3 (left) and we obtain

$$\nu = 1.05 \pm 0.05. \tag{7}$$

This estimate for ν lies between the value of the two- and three-dimensional bond percolation [11].

The analysis of the average number of percolating loops $N_L^{\text{perco}}(p)$, obeying a similar finite-size scaling form $N_L^{\text{perco}}(p) = \tilde{N}^{\text{perco}}[(\sigma - \sigma_c)L^{1/\nu}]$ gives the same estimates for σ_c and ν (cf figure 3 (right)). Note that at σ_c the average number of percolating loops does not (or only weakly) depend on the system size and is small: $N_L^{\text{perco}}(p_c) \approx 0.3$. The maximum number of percolating loops we observed for $L = 32$ at σ_c was three with a very low probability.

The average mass m of a percolating loop at σ_c scales with L like

$$m \sim L^{d_f} \tag{8}$$

where d_f is a fractal dimension. For $\sigma = \sigma_c$ we get with the data shown in figure 4

$$d_f = 1.64 \pm 0.04. \tag{9}$$

The probability P_∞ that a bond belongs to a percolating loop is expected to scale like

$$P_\infty \sim L^{-\beta/\nu} \; \tilde{P}_\infty[(\sigma - \sigma_c)L^{1/\nu}]. \tag{10}$$

The figure 4 (right) shows the raw data of P_∞ (inset) and the plot of the scaling law (10) with $\nu = 1.05 \pm 0.05$ and $\beta/\nu = 1.3 \pm 0.1$, i.e.

$$\beta = 1.4 \pm 0.1. \tag{11}$$

The usual hyperscaling relation, $\beta/\nu = d - d_f$, known from conventional percolation [11] gives $d_f = 1.6 \pm 0.1$, which is consistent with (9).

The loop distribution function n_m, i.e. the average number n_m of finite loops of mass m per lattice bond, obeys the scaling form (in the limit $L \to \infty$)

$$n_m \sim m^{-\tau} \; \tilde{n}_m[(\sigma - \sigma_c)\,m^s] \tag{12}$$

where τ is the Fisher exponent and s another critical exponent (usually denoted σ in conventional percolation, which we avoid due to possible confusion with the disorder
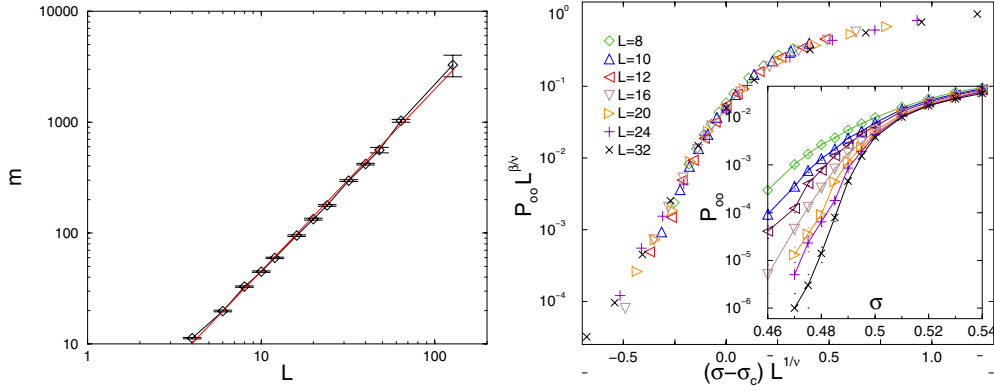
Figure 4. Left: plot of the average mass m of a percolating loop versus L for $\sigma = \sigma_c$. The error bars are smaller than the symbols. The straight line is a least-squares fit to $m \sim L^{L^{d_f}}$ giving $d_f = 1.64 \pm 0.04$. Right: finite-size scaling plot of the probability P_∞ for a bond belonging to a percolating loop for different system size L with $\sigma_c = 0.495$, $\nu = 1.05$ and $\beta/\nu = 1.3$. The inset shows a lin–log plot of the raw data.
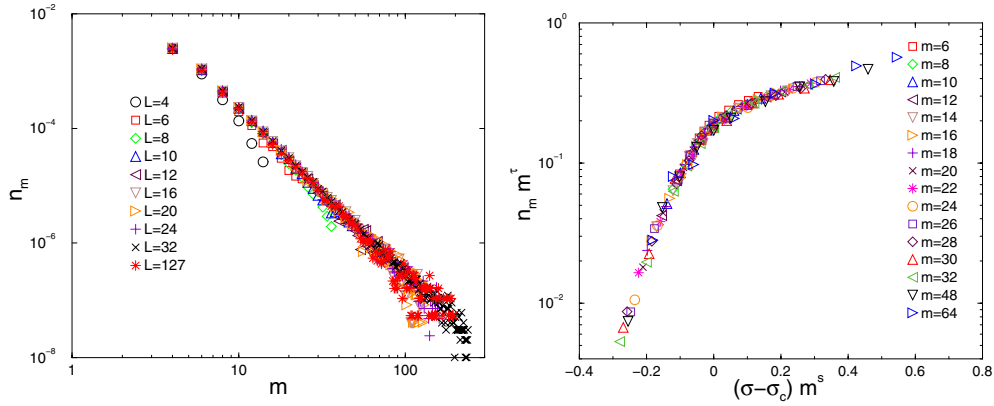
Figure 5. Left: probability distribution n_m at $\sigma = \sigma_c$ for different system size L. A least-squares fit to $n_m \sim m^{-\tau}$ yields $\tau = 2.8 \pm 0.1$. Right: finite-size scaling of n_m for $L = 32$ with $\sigma_c = 0.495$, $s = 0.6$ and $\tau = 2.95$. For $m \geqslant 30$ the statistics is over fewer than 1000 loops for each σ.

strength σ). The exponent s describes how fast the number of loops of mass m decreases as a function of m close to σ_c. Figure 5 (left) shows the raw data of n_m for different L and $\sigma = \sigma_c$. For $L = 32$ we get $\tau = 2.89 \pm 0.05$ and for $L = 127$ (three samples) $\tau = 2.84 \pm 0.06$. In the limit $L \to \infty$ we expect
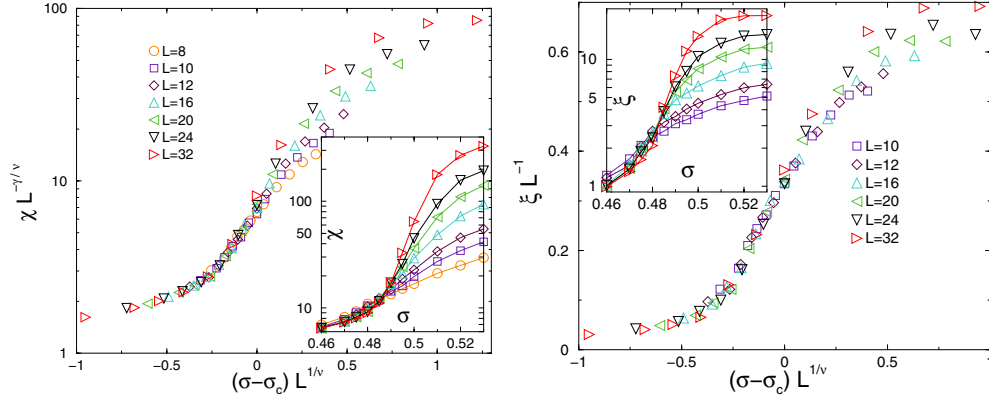
$$\tau = 2.8 \pm 0.1. \tag{13}$$

From the finite-size scaling plot of equation (12), we get $\tau = 2.95 \pm 0.05$ and

$$s = 0.6 \pm 0.1 \tag{14}$$

for $\sigma_c = 0.495 \pm 0.005$ and $L = 32$ in figure 5 (right).

The zeroth moment $n = \sum_m n_m$ represents the average number of loops per bond. Below σ_c the data collapse and satisfy $n \sim \sigma$. The average loop size, defined as the ratio of the second

Figure 6. Left: finite-size scaling plot of the susceptibility χ for $\sigma_c = 0.495$, $\nu = 1.05$ and $\gamma/\nu = 0.42$. Right: scaling plot of the correlation length ξ for $\sigma_c = 0.495$ and $\nu = 1.05$. The inset shows the raw data.

and first moment of the loop distribution [11]

$$\chi := \left(\sum_{m=4}^{\infty} m^2 n_m \right) \Big/ \left(\sum_{m=4}^{\infty} m\, n_m \right) \tag{15}$$

is expected to scale like

$$\chi \sim L^{\gamma/\nu} \, \tilde{\chi}[(\sigma - \sigma_c)L^{1/\nu}]. \tag{16}$$

The data in figure 6 (left) show the raw data (inset) and verify the scaling law (16) with $\gamma/\nu = 0.4 \pm 0.1$ for $\sigma_c = 0.495$ and $\nu = 1.05 \pm 0.05$, i.e

$$\gamma = 0.4 \pm 0.1. \tag{17}$$

The above estimates for γ (17) and β (11) together with those for τ (13) and s (14) fulfil the usual exponent relation known from conventional percolation

$$\gamma = \frac{3 - \tau}{s} \qquad \beta = \frac{\tau - 2}{s}. \tag{18}$$

Near σ_c the linear size of a finite loop is characterized by the correlation length ξ, which we calculate with the help of the radius R_{m_i} of gyration for the loop i of mass m_i defined as

$$R_{m_i}^2 := \frac{1}{m_i} \sum_{j=1}^{m_i} |\boldsymbol{r}_{ji} - \boldsymbol{r}_{0i}|^2 \qquad \text{with} \quad \boldsymbol{r}_{0i} := \frac{1}{m_i} \sum_{j=1}^{m_i} \boldsymbol{r}_{ji} \tag{19}$$

where $\boldsymbol{r}_{ji}$ is the position of a bond j of the loop i and $\boldsymbol{r}_{0i}$ the centre of mass. Then, the correlation length ξ is defined by

$$\xi^2 := \left(\sum_{m=4}^{\infty} R_m^2 m^2 n_m \right) \Big/ \left(\sum_{m=4}^{\infty} m^2 n_m \right) \tag{20}$$

where R_m is the average radius of gyration of loops of mass m (averaged over disorder and individual loops). The raw data of ξ are shown in the inset of figure 6 (right). The finite-size scaling form for ξ is

$$\xi \sim L \tilde{\xi}[(\sigma - \sigma_c)L^{1/\nu}]. \tag{21}$$

From the best data collapse we get $\nu = 1.05 \pm 0.05$, as shown in figure 6 (right), consistent with (7).
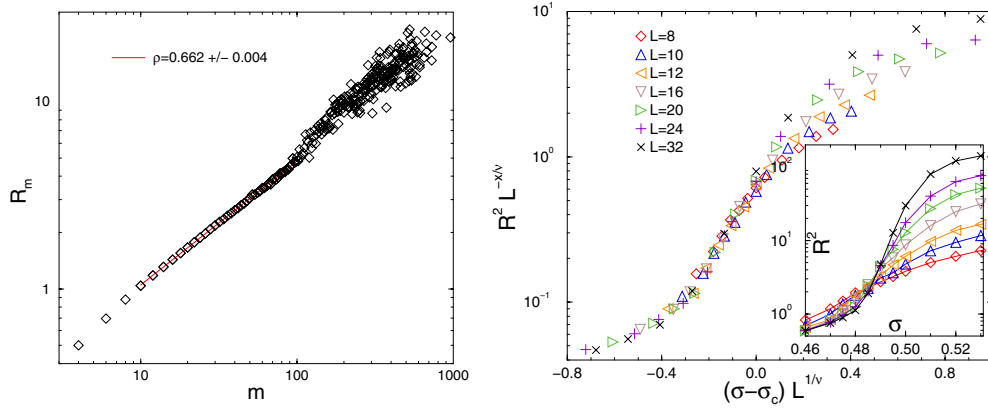
Figure 7. Left: average radius of gyration R_m versus the mass m at $\sigma = \sigma_c$ for 1000 samples and $L = 32$. A least-squares fit to $R_m \sim m^\rho$ yields $\rho = 0.66 \pm 0.04$. Right: finite-size scaling of the square loop radius of R^2 for different system sizes L with $\sigma_c = 0.492$, $\nu = 1.05$ and $x/\nu = 0.8$. The inset shows the raw data.

At the percolation threshold the average radius of gyration R_m of a loop of mass m increases algebraically

$$R_m \sim m^\rho. \tag{22}$$

In figure 7 (left) we plot R_m for $\sigma = \sigma_c$ and fit the data in the interval $m \in \{10, \ldots, 100\}$ to the power law (22), which yields

$$\rho = 0.66 \pm 0.04 \qquad \text{or} \quad d_f = 1/\rho = 1.5 \pm 0.1 \tag{23}$$

which agrees with our previous estimate for the fractal dimension d_f of the percolating loops (9) within the error bars.

Another quantity, which characterizes the size of finite loops, is the mean square radius R^2, defined as

$$R^2 := \left(\sum_{m=4}^{\infty} R_m^2 \, m \, n_m \right) \Big/ \left(\sum_{m=4}^{\infty} m \, n_m \right). \tag{24}$$

We expect R^2 to scale like

$$R^2 \sim L^{x/\nu} \, \tilde{R}[(\sigma - \sigma_c)L^{1/\nu}] \tag{25}$$

where x is another critical exponent. As depicted in figure 7 (right) for the best data collapse we get $x/\nu = 0.8 \pm 0.1$ with $\nu = 1.05 \pm 0.05$ (and $\sigma_c = 0.495 \pm 0.005$), i.e.

$$x = 0.8 \pm 0.1. \tag{26}$$

This exponent should fulfil the relation [11]

$$x = 2\nu - \beta. \tag{27}$$

With ν from (7) and β from (11) we get $x = 0.7 \pm 0.2$, which is consistent with (26).

5. Summary

In summary, we studied the ground state of the three-dimensional strongly screened vortex glass model numerically. We found a clear evidence for a disorder-driven

superconducting-to-normal phase transition indicated by a change in the stiffness exponent at σ_c. This transition turned out to be a percolation transition for disorder-induced vortex loops crossing the whole system.

At first sight it might seem surprising that the existence of percolating vortex loops is related to a change in the stiffness exponent of model (1). However, the stiffness exponent provides information on how hard it is to induce a domain wall into a system of linear size L and a domain wall is surrounded by a global vortex loop. If, at and above a critical disorder strength, global vortex loops already proliferate in the ground state, the creation of an extra excitation loop will, with probability 1, cost only an infinitesimal amount of energy in the limit of infinite system size.

A similar observation—the coincidence of vortex loop percolation and a thermal phase transition in superconductors—has been made earlier in models for high-T_c superconductors. In [13] it was shown for a model of a *pure* superconductor that the melting transition of the Abrikosov flux line lattice at the temperature T_{c2} where the transition from the superconductor to normal phase takes place is accompanied by a proliferation of thermally induced global vortex loops. And similarly in [14] it was shown that the temperature-driven resistivity transition in disordered high-T_c superconductors is also accompanied by a percolation transition of vortex lines perpendicular to the applied field. These thermally induced transitions are, however, in universality classes different from the disorder-induced transition that we have studied here.

Acknowledgments

References

[1] Ebner C and Stroud D 1985 *Phys. Rev.* B **31** 165
    John S and Lubensky T C 1986 *Phys. Rev.* B **34** 4815
[2] Fisher M P A 1989 *Phys. Rev. Lett.* **62** 1415
    Fisher D S, Fisher M P A and Huse D A 1991 *Phys. Rev.* B **43** 130
    Fisher M P A, Tokuyasu T A and Young A P 1991 *Phys. Rev. Lett.* **66** 2931
[3] Reger J D, Tokuyasu T A, Young A P and Fisher M P A 1991 *Phys. Rev.* B **44** 7147
    Gingras M J P 1992 *Phys. Rev.* B **45** 7547
    Maucourt J and Grempel D R 1998 *Phys. Rev. Lett.* **80** 770
[4] Bokil H S and Young A P 1995 *Phys. Rev. Lett.* **74** 3021
[5] Kosterlitz J M and Simkin M V 1997 *Phys. Rev. Lett.* **79** 1098
[6] Kisker J and Rieger H 1998 *Phys. Rev.* B **58** R8873
[7] Kleinert H 1989 *Gauge Fields in Condensed Matter I + II* (Singapore: World Scientific)
    Le Bellac M 1991 *Quantum and Statistical Field Theory* (Oxford: Oxford University Press)
[8] Rieger H 1998 *Lecture Notes in Physics* vol 501, ed J Kertesz and I Kondor (Berlin: Springer) pp 122–58
    Alava M, Duxbury P, Moukarzel M and Rieger H 2001 Combinatorial optimization and disordered systems
        Phase Transition and Critical Phenomena vol 18, ed C Domb and J L Lebowitz (Cambridge, MA: Cambridge
        Academic) pp 141–317
    Hartmann A and Rieger H 2001 *Optimization Algorithms in Physics* (Berlin: Wiley-VCH)
[9] Pfeiffer F O and Rieger H 1999 *Phys. Rev.* B **60** 6304
[10] Wengel C and Young A P 1996 *Phys. Rev.* B **54** R6869
[11] Stauffer D 1985 *Introduction to Percolation Theory* (London: Taylor and Francis)
    Bunde A and Havlin S 1996 *Fractals and Disordered Systems* 2nd edn (Berlin: Springer)
[12] Grassberger P 1992 *J. Phys. A: Math. Gen.* **25** 5867
[13] Nguyen A K and Sudbø A 1998 *Phys. Rev.* B **58** 2802
[14] Jagla E A and Balseiro C A 1996 *Phys. Rev.* B **53** 15 305